International Journal of Thermal Sciences 48 (2009) 1619–1626

Contents lists available at ScienceDirect

International Journal of Thermal Sciences

www.elsevier.com/locate/ijts

Transient mixed convection flow arising due to thermal diffusion over a porous sensor surface inside a squeezing horizontal channel

M. Mahmood, S. Asghar, M.A. Hossain *,[1]

Department of Mathematics, COMSATS Institute of Information Technology, 30, Sector H-8/1, Islamabad, Pakistan

ARTICLE INFO

Article history:
Received 5 February 2008
Received in revised form 13 December 2008
Accepted 16 December 2008
Available online 10 March 2009

Keywords:
Mixed convection
Horizontal surface
Squeezed flow

ABSTRACT

A transient laminar mixed convection flow of viscous incompressible fluid generated by thermal buoyancy force, over a horizontal porous sensor surface placed inside a squeezing channel is analysed. The non-similar boundary layer equations for the flow and energy are solved numerically for different time regimes. The quantities of physical interest like skin friction coefficient, heat transfer coefficient, velocity and temperature profiles are calculated for different values of physical parameters, Pr, b, S and ξ. The implicit finite difference approximation together with Keller box method is employed for the solution for small and all time regime, where as, a series solution is found for large time regimes. A good agreement of the results computed by different methods has been observed.

1. Introduction

The buoyancy force, resulting from flow over a horizontal surface gives rise to a hydrostatic pressure distribution across the boundary layer. This hydrostatic pressure modifies the forced convection boundary layer to a greater extent, depending upon the temperature of the heated surface. If the temperature of the surface is higher than the ambient temperature, the induced pressure gradient due to buoyancy force results in an aiding flow, whereas if the temperature of the surface is below the ambient temperature, this results is an opposing flow.

The mixed convection on the horizontal surface due a uniform free stream, has been studied by many workers. Mori [1] considered the weakly buoyant flows by expanding the variables in terms of direct coordinate expansion valid in a region near the leading edge of the plate. He presented numerical solution for the first order perturbations. Sparrow and Minkowycz [2] not only corrected some minor errors in the solution by [1], but also presented the solution for a relatively wider range of Pr number. Hieber [3] studied the strongly buoyant flows in terms of inverse coordinate expansion and the solution of first three terms in the inverse expansion was presented for $Pr = 0.72$. The two expansions direct or indirect fail to describe the entire mixed convection regime, specially in the region where mixed convection effects are moderate. For limiting Pr numbers, the solution of the equations for direct and indirect expansions was presented by Hieber [3] and Leal [4]. Approximate solutions for the modified boundary layer equations was presented by Martynenko and Sokovishin [5] using an integral method similar to Karman–Pohlhausen. Chen et al. [6] and Mocoglu and Chen [7] have studied the problem with local non-similarity and related methods. The experimental results for mixed, free and forced convection, for air, were presented by Wang [8]. The vortex instability of mixed convection flow for a horizontal surface cooled from above, was presented by Moutsoglou et al. [9]. Pera and Gebhart [10] presented the solution of Navier–Stokes equation for the flow over an inclined surface using the method of series truncation. A particular self similar solution of the mixed convection flow over a horizontal surface was presented by Schneider [11] for the case of specified wall temperature as an inverse square root of the distance form the leading edge. Later, Raju et al. [12] and Schneider and Wasel [13] studied the cases of prescribed heat flux and prescribed wall temperature by integrating the boundary layer equations using finite difference technique. Raju et al. [12] and Noor Afzal [14] presented a solution for the entire mixed convection domain, showing a smooth transition from one convection limit to other. The boundary-layer flow over a cooled horizontal plate is considered by Steinrück [15]. It is shown that the real part of the spectrum of the evolution operator of the linearised equations is not bounded uniformly from above, which explains the difficulties encountered by a numerical solution. Furthermore, it is shown that near the leading edge an asymptotic expansion of the solution is not unique. Later, the two-dimensional boundary-layer flow over a cooled/heated flat plate is investigated by Denier et al. [16]. A cooled plate (with a free-stream flow and wall temperature distribution which admit similarity solutions) is shown to support non-modal disturbances, which grow algebraically with distance downstream from the leading edge of the

* Corresponding author.
E-mail addresses: anwar@univdhaka.edu, cfd@bdcom.com, drma_hossain@yahoo.com (M.A. Hossain).
[1] Professor of Mathematics (Rtd), University of Dhaka, Dhaka 1000, Bangladesh.

1290-0729/$ – see front matter
doi:10.1016/j.ijthermalsci.2008.12.009

Nomenclature

a	squeeze flow strength
b	index of the squeeze flow
S	porosity parameter
f	dimensionless stream function
$h(t)$	height of the channel
u	axial velocity
v	normal velocity
p	pressure distribution
p_∞	free stream pressure distribution
x	axial distance
k	fluid thermal conductivity
Nu	Nusselt number
Pr	Prandtl number
Re	free stream Reynolds number
Re_c	cross flow Reynolds number
Gr	Grashof number
T	fluid temperature
T_0	reference planner temperature distribution
T_∞	free stream temperature
T_w	surface temperature
t	time
U	free stream velocity
y	normal distance
g	gravitational acceleration
V_0	injection/suction velocity
α	fluid thermal diffusivity
η	similarity transformation in terms of y and t
μ	fluid dynamic viscosity
θ	dimensionless fluid temperature
ρ	fluid density
ν	kinematic viscosity
ψ	stream function
ξ	mixed convection parameter
β_T	coefficient of thermal expansion
τ_w	shear stress at the surface

plate. Recently, Mahmood et al. [17], studied the flow and heat transfer, over a horizontal surface inside a squeezing channel. The effect of buoyancy force was not included in this study.

In this work we investigate the unsteady mixed convective boundary layer flow over a porous, horizontal sensor surface inside a squeezing horizontal channel. The set of equations that govern the flow are reduced to a set of parabolic partial differential equations, solutions of which are obtained numerically over all range of time for the case of impermeable as well as permeable sensor surface. The implicit finite difference method is employed for the solution of small and large time regimes. Asymptotic series solution is also found for large time regimes. Finally, the results are presented in the form of transient skin-friction and Nusselt number for fluids having Prandtl number, Pr, equal to 0.71 (air 20 °C at 1 atm.), 1.02 (water vapour at 140 °C), 6.7 (saturated water at 22 °C) and 9.4 (water at 10 °C). Velocity profiles and the temperature profiles, for the same values of Pr, have also been presented graphically. Finally, numerical values obtained for small and large time regimes being compared with the solutions obtained for all time regimes found in excellent agreement.

2. Mathematical formulation

Consider the unsteady boundary layer flow of viscous incompressible fluid over a horizontal porous sensor surface inside a squeezing horizontal channel. The squeezing takes place as a function of time, only at the upper surface of the channel. The height of the channel is much greater than the boundary layer thickness. The height $h(t)$ is the separation between the edge of boundary layer and the channel upper surface, which decreases as time increases. The x-axis is along the porous surface starting from its free end and y-axis is normal to it as shown in Fig. 1. The flow is driven by the combined effect of thermal buoyancy and an external free stream $U(x,t)$. The temperature of the free stream is assumed to be constant, T_∞, whereas, the horizontal surface is maintained at a non-uniform temperature, $T_w(x)$.

Under the usual Boussinesq approximation, following are the boundary layer equations for the flow in the dimensional form are

$$\frac{\partial u}{\partial x}+\frac{\partial v}{\partial y}=0, \tag{1}$$

$$\frac{\partial u}{\partial t}+u\frac{\partial u}{\partial x}+v\frac{\partial u}{\partial y}=-\frac{1}{\rho}\frac{\partial p}{\partial x}+\nu\frac{\partial^2 u}{\partial y^2}, \tag{2}$$

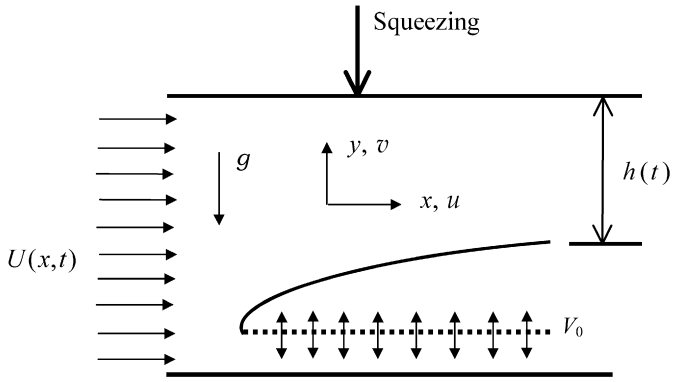

Fig. 1. Flow configuration and coordinate system.

$$0=-\frac{1}{\rho}\frac{\partial p}{\partial y}+g\beta_T(T-T_\infty), \tag{3}$$

$$\frac{\partial T}{\partial t}+u\frac{\partial T}{\partial x}+v\frac{\partial T}{\partial y}=\alpha\frac{\partial^2 T}{\partial y^2}, \tag{4}$$

where, u, v, t, T, ν and p are the x-component of velocity, y-component of velocity, time, temperature, kinematic viscosity and the pressure. Also α is the thermal diffusivity, g is the acceleration due to gravity, ρ is the density and β_T is the coefficient of thermal expansion.

The subjected initial and boundary conditions are:

For $t \leqslant 0$

$$u(x,0)=0, \qquad v(x,0)=-V_0, \qquad T(x,0)=T_w(x),$$
$$u(x,\infty)=U(x), \qquad T(x,\infty)=T_\infty, \qquad p(x,\infty)=p_\infty(x).$$

For $t>0$

$$u(x,0,t)=0, \qquad v(x,0,t)=-V_0,$$
$$T(x,0,t)=T_w(x), \qquad u(x,\infty,t)=U(x,t),$$
$$T(x,\infty,t)=T_\infty, \qquad p(x,\infty,t)=p_\infty(x,t), \tag{5}$$

where $T_w(x)=T_0x^2+T_\infty$ is the variable temperature of the heated surface, T_0 is some reference planer temperature distribution, V_0 is the suction/injection velocity, that is positive for injection and negative for the case of suction through the porous

surface. The free stream pressure distribution $p_\infty(x,t)$ can be written as following, using the Euler's equation

$$p_\infty(x,t) = \frac{U_0 x^2}{2(1+bt)^2}(b - U_0). \tag{6}$$

The free stream velocity, following Khaled and Vafai [18], is taken of the form

$$U(x,t) = \frac{U_0 x}{(1+bt)}, \tag{7}$$

where, U_0 and b are constants. The variable height above the edge of boundary layer is of the form $h(t) = h_0/(1+bt)$, where h_0 is a constant. For t approaching infinity, the free stream velocity tends to zero and the height $h(t)$ is also zero. At this time, the channel upper surface is at the edge of natural convection boundary layer. We can see that for the case, $b = 0$ (no squeezing), the free stream is only a function of x and for non-zero value of b, the free stream velocity decreases as time lapses. Here, we can see that for the case, $b = 0$, the flow refers to an unsteady stagnation point flow past a horizontal surface. The free stream defined in Eq. (7) is valid only for $x > 0$, whereas $x = 0$ is the stagnation point for the flow at which, the flow is only the natural convection flow.

3. Transformations and methods of solution

Here, we propose the appropriate group of transformations for different time regimes, *i.e.*, small, large, and entire time regimes and discuss the methods of solution of the transformed equations.

3.1. Small time regime

We can see from Eq. (7), that for small time, the potential flow is very strong and it dominates the flow. We can thus, term the flow in this time regime as the forced convection flow. The following dependent and independent variables are defined for this time regime.

$$\psi = \nu Re^{1/2} f(\eta,\xi), \qquad \eta = \frac{y}{x} Re^{1/2},$$
$$\theta(\eta,\xi) = \frac{(T - T_\infty)}{(T_w(x) - T_\infty)}, \qquad \xi = \frac{Gr}{Re^{5/2}},$$
$$p = p_\infty(x,t) + \frac{\rho\nu^2}{x^3}\frac{Gr}{Re^{1/2}} h(\eta,\xi), \tag{8}$$

where, Re $(= Ux/\nu)$ is the local as well as the instantaneous Reynolds number, $Gr = g\beta_T(T_w(\bar{x}) - T_\infty)x^3/\nu^2$ is the Grashof number, due to the effect of thermal buoyancy force. The parameter ξ $(= Gr/Re^{5/2})$ may be termed as the mixed convection parameter, depending upon time, provided that $b \neq 0$. For $b = 0$, it represents mixed convection parameter for the unsteady stagnation point flow. This parameter measures the relative strength of the buoyancy forces to the inertial forces. The minimum value of ξ, is zero for the case when no buoyancy force is considered. Whereas, for very small value of ξ, the effect of buoyancy force on the flow field is very small in comparison to the inertial force. This refers to the forced convection flow. Similarly, large value of ξ refers to natural convection flow, when the buoyancy force is very large, when compared with the inertial force. The intermediate range of ξ, refers to the mixed convection regime, when both the buoyancy and inertial forces are of comparative scale. Simultaneously, for a fix value of Gr, the small or large value of ξ, represents small or large time, provided $b \neq 0$.

Now, substituting the transformation (8) into the set of Eqs. (1) to (5), we obtain the following locally non-similar equations

Table 1
Numerical values of $\frac{1}{2}Re^{1/2}C_f$ and $Re^{-1/2}Nu$ for different range of ξ when $Pr = 0.71$, $S = 0$.

ξ	$b = 0.2$		$b = 0.5$	
	Small/large ξ	IFD	Small/large ξ	IFD
0.0	1.14972	1.17462	1.07223	1.08441
0.3	1.30872	1.35699	1.23765	1.24542
0.5	1.43763	1.46841	1.35801	1.35044
1.0	1.70765	1.73479	1.59021	1.58951
2.5	–	2.41273	–	2.23970
10.0	–	4.92491	–	4.65680
20.0	–	7.34939	–	7.06780
40.0	–	11.08927	–	10.81757
60.0	–	14.14685	–	14.02742
80.0	–	16.83987	–	16.56248
90.0	–	18.08347	–	17.81800
95.0	18.39926	18.67324	18.24757	18.41974
98.0	18.95133	19.02120	18.59869	18.77484
99.0	19.06774	19.13625	18.71479	18.89225
100.0	19.19836	19.23940	18.83042	19.00920

$$f''' + ff'' - f'^2 + bf' + \frac{1}{2}b\eta f'' + 1 - b - 2\xi h = \frac{5}{2}b\xi\frac{\partial f'}{\partial \xi}, \tag{9}$$

$$h' = \theta, \tag{10}$$

$$\frac{1}{Pr}\theta'' - 2f'\theta + f\theta' + \frac{1}{2}b\eta\theta' = \frac{5}{2}b\xi\frac{\partial\theta}{\partial\xi}. \tag{11}$$

The corresponding boundary conditions to be satisfied by the above equations, become

$$f(0,\xi) = S\xi^{1/5}, \qquad f'(0,\xi) = 0, \qquad \theta(0,\xi) = 1,$$
$$f'(\infty,\xi) = 1, \qquad \theta(\infty,\xi) = 0, \qquad h(\infty,\xi) = 0, \tag{12}$$

where, Pr $(= \nu/\alpha)$ is the Prandtl number and S $(= -Re_c/Gr^{1/5})$ is the porosity parameter and Re_c $(= V_0 x/\nu)$ is the cross flow Reynolds number.

In practical applications, two quantities of physical interest are to be determined, which are, surface shear stress and heat transfer at the surface. These may be obtained in terms of skin-friction C_f, and Nusselt number, Nu, from the following relation

$$C_f = \frac{2\tau_w(x)}{\rho U^2}, \qquad Nu = \frac{q_w x}{k(T_w - T_\infty)}, \tag{13}$$

where $\tau_w = \mu(\partial u/\partial y)_{y=0}$ is the shear stress at the surface and $q_w = -k(\partial T/\partial y)_{y=0}$ is the heat flux at the surface.

Now, the non-dimensional quantities, skin-friction coefficient, $1/2C_f Re^{1/2}$ and the heat transfer coefficient $Nu\,Re^{-1/2}$, may be obtained from the following expressions

$$\frac{1}{2}Re^{1/2}C_f = f''(0,\xi),$$
$$Re^{-1/2}Nu = -\theta'(0,\xi). \tag{14}$$

The solution of the set of Eqs. (9) to (12) is obtained using perturbation method by expanding the dependent variables in powers of ξ. Since, the solution thus obtained not found comparable with that obtained by other methods, for value of ξ greater than 0.01, here we have simulated the set of Eqs. (9) to (12) employing the implicit finite difference. The detail of this method will be discussed in the following section. The results thus obtained for skin friction coefficient and heat transfer coefficient, are presented in Tables 1 and 2, respectively, for values of $Pr = 0.71$, $S = 0.0$, $b = 0.2$ and $b = 0.5$, for $\xi \in [0, 1]$.

3.2. Large time regime

It can be seen from Eq. (7) that at large time, the potential flow U, tends to zero and the flow develops solely due to the presence of buoyancy force, arising due to thermal diffusion from the

Table 2
Numerical values of $\frac{1}{2}Re^{1/2}C_f$ and $Re^{-1/2}Nu$ for different range of ξ when $Pr = 0.71$, $S = 0$.

ξ	$b = 0.2$		$b = 0.5$	
	Small/large ξ	IFD	Small/large ξ	IFD
0.0	0.86074	0.86904	0.88258	0.88766
0.3	0.88901	0.89562	0.89856	0.90712
0.5	0.90935	0.91050	0.92012	0.92368
1.0	0.94128	0.94394	0.94892	0.95786
2.5	–	1.01846	–	1.03126
10.0	–	1.23571	–	1.23386
20.0	–	1.39459	–	1.38751
40.0	–	1.58538	–	1.57732
60.0	–	1.71274	–	1.71060
80.0	–	1.81026	–	1.80304
90.0	–	1.85221	–	1.84564
95.0	1.84504	1.87213	1.84883	1.86536
98.0	1.85644	1.88369	1.86020	1.87681
99.0	1.86018	1.88748	1.86393	1.88057
100.0	1.86388	1.89086	1.86763	1.88429

heated horizontal surface. In order to obtain a system of equations applicable to large time regime, we define following set of dependent and independent variables

$$\psi = \nu Re^{1/2}\xi^{1/5}\bar{f}(\eta,\xi), \qquad \bar{\eta} = \frac{y}{x}\xi^{1/5}Re^{1/2},$$
$$\theta(\eta,\xi) = \frac{(T-T_\infty)}{(T_w-T_\infty)},$$
$$p = p_\infty(x,t) + \frac{\rho\nu^2}{x^3}\frac{Gr}{Re^{5/2}}\xi^{-1/5}\bar{h}(\eta,\xi). \tag{15}$$

After substituting (15) into Eqs. (9) to (12), we get

$$\bar{f}''' + \bar{f}\bar{f}'' - \bar{f}'^2 + \xi^{-2/5}\frac{1}{2}b\bar{\eta}\bar{f}'' + \xi^{-4/5}(1-b) - 2\bar{h} = \xi^{3/5}\frac{5}{2}b\frac{\partial\bar{f}'}{\partial\xi}, \tag{16}$$
$$\bar{h}' = \bar{\theta}, \tag{17}$$
$$\frac{1}{Pr}\bar{\theta}'' - 2\bar{f}'\bar{\theta} + \bar{f}\bar{\theta}' + \xi^{-2/5}\frac{1}{2}b\bar{\eta}\bar{\theta}' = 0, \tag{18}$$
$$\bar{f}(0,\xi) = S, \qquad \bar{f}'(0,\xi) = 0, \qquad \bar{\theta}(0,\xi) = 1,$$
$$\bar{f}'(\infty,\xi) = \xi^{-2/5}, \qquad \bar{\theta}(\infty,\xi) = 0, \qquad \bar{h}(\infty,\xi) = 0. \tag{19}$$

An asymptotic series solution is proposed for Eqs. (16) to (19). The boundary conditions in (19) suggest the following series expansion for the functions $\bar{f}, \bar{\theta}$, and $\bar{h}$.

$$\bar{f}(\bar{\eta},\xi) = \sum_{i=0}^{\infty}\xi^{-2i/5}\bar{f}_i(\bar{\eta},\xi),$$
$$\bar{\theta}(\bar{\eta},\xi) = \sum_{i=0}^{\infty}\xi^{-2i/5}\bar{\theta}_i(\bar{\eta},\xi),$$
$$\bar{h}(\bar{\eta},\xi) = \sum_{i=0}^{\infty}\xi^{-2i/5}\bar{h}_i(\bar{\eta},\xi). \tag{20}$$

Substituting (20) into Eqs. (16) to (19) and equating the powers of ξ, we obtain the equations for successive approximations. The system of equations for leading order, turn out to be

$$\bar{f}_0''' + \bar{f}_0\bar{f}_0'' - \bar{f}_0'^2 - 2\bar{h}_0 = 0, \tag{21}$$
$$\bar{h}_0' = \bar{\theta}_0, \tag{22}$$
$$\frac{1}{Pr}\bar{\theta}_0'' - 2\bar{f}_0'\bar{\theta}_0 + \bar{f}_0\bar{\theta}_0' = 0, \tag{23}$$
$$\bar{f}_0(0) = S, \qquad \bar{f}_0'(0) = 0, \qquad \bar{\theta}_0(0) = 1,$$
$$\bar{f}_0'(\infty) = 0, \qquad \bar{\theta}_0(\infty) = 0, \qquad \bar{h}_0(\infty) = 0. \tag{24}$$

Here, it is very interesting to note that Eqs. (21) to (24), represent the equations for purely steady natural convection flow along a horizontal heated surface. We can say here that starting from a forced convection for small time, the flow transforms to a purely natural convection flow at extremely large time, where the flow becomes steady natural convection flow.

Next, the first order system appears as

$$\bar{f}_1''' + \bar{f}_0\bar{f}_1'' + \bar{f}_1\bar{f}_0'' - 2\bar{f}_0'\bar{f}_1' + \frac{1}{2}b\bar{\eta}\bar{f}_0 - 2\bar{h}_1 = 0, \tag{25}$$
$$\bar{h}_1' = \bar{\theta}_1, \tag{26}$$
$$\frac{1}{Pr}\bar{\theta}_1'' - 2(\bar{f}_0'\bar{\theta}_1 + \bar{f}_1'\bar{\theta}_0) + \bar{f}_0\bar{\theta}_1' + \bar{f}_1\bar{\theta}_0' + \frac{1}{2}b\bar{\eta}\bar{\theta}_0' = 0, \tag{27}$$
$$\bar{f}_1(0) = 0, \qquad \bar{f}_1'(0) = 0, \qquad \bar{\theta}_1(0) = 0,$$
$$\bar{f}_1'(\infty) = 1, \qquad \bar{\theta}_1(\infty) = 0, \qquad \bar{h}_1(\infty) = 0. \tag{28}$$

The leading order and the first order systems thus obtained, are solved numerically using Newton–Raphson technique method together with sixth-order implicit Runge–Kutta method.

The physical quantities like, skin friction and the Nusselt number, can then be calculated using the following relations:

$$\frac{1}{2}Re^{1/2}C_f = \xi^{3/5}\left\{\bar{f}_0''(0) + \xi^{-2/5}\bar{f}_1''(0) + O\left(\xi^{-4/5}\right)\right\},$$
$$Re^{-1/2}Nu = -\xi^{1/5}\left\{\bar{\theta}_0'(0) + \xi^{-2/5}\bar{\theta}_1'(0) + O\left(\xi^{-4/5}\right)\right\}. \tag{29}$$

For example, taking $Pr = 0.71$ and $b = 0.5$, the values of $\bar{f}_0''(0)$, $\bar{f}_1''(0)$, $\bar{\theta}_0'(0)$ and $\bar{\theta}_1'(0)$ are obtained using which the numerical values of the skin friction coefficient, $\frac{1}{2}Re^{1/2}C_f$, and heat transfer coefficient, $Re^{-1/2}Nu$, can be obtained for different values of ξ, from

$$\frac{1}{2}Re^{1/2}C_f = \xi^{3/5}\left\{1.22626 + (\xi)^{-2/5}(-0.24067)\right\},$$
$$Re^{-1/2}Nu = -\xi^{1/5}\left\{-0.73859 + (\xi)^{-2/5}(-0.03108)\right\}. \tag{30}$$

Values of the skin friction, $\frac{1}{2}Re^{1/2}C_f$, and the Nusselt number, $Re^{-1/2}Nu$ are obtained for ξ in the range [90, 100]. These values are entered in Tables 1 and 2 for comparison with those obtained by the implicit finite difference method for entire regime of ξ.

3.3. Entire time regime

Looking at the set of Eqs. (9) to (12) and (16) to (19) the appropriate scaling for all time regime can be proposed as

$$\psi = \nu Re^{1/2}(1+\xi)^{1/5}\tilde{f}(\tilde{\eta},\xi),$$
$$\tilde{\eta} = \frac{y}{x}(1+\xi)^{1/5}Re^{1/2}, \qquad \theta(\tilde{\eta},\xi) = \frac{(T-T_\infty)}{(T_w-T_\infty)},$$
$$p = p_\infty(x,t) + \frac{\rho\nu^2}{x^3}\frac{Gr}{Re^{5/2}}(1+\xi)^{-1/5}\tilde{h}(\tilde{\eta},\xi). \tag{31}$$

The corresponding equations (9) to (12) thus take the form

$$\tilde{f}''' + \tilde{f}\tilde{f}'' - \tilde{f}'^2 + (1+\xi)^{-2/5}\left\{\frac{b\tilde{f}'}{1+\xi} + \frac{1}{2}b\tilde{\eta}\tilde{f}''\right\} + (1+\xi)^{-4/5}(1-b) - \frac{\xi}{1+\xi}2\tilde{h} = \xi(1+\xi)^{-2/5}\frac{5}{2}b\frac{\partial\tilde{f}'}{\partial\xi}, \tag{32}$$
$$\tilde{h}' = \tilde{\theta}, \tag{33}$$
$$\frac{1}{Pr}\tilde{\theta}'' - 2\tilde{f}'\tilde{\theta} + \tilde{f}\tilde{\theta}' + (1+\xi)^{-2/5}\frac{1}{2}b\tilde{\eta}\tilde{\theta}' = \xi(1+\xi)^{-2/5}\frac{5}{2}b\frac{\partial\tilde{\theta}}{\partial\xi}, \tag{34}$$

$$\tilde{f}(0,\xi) = S\left(\frac{\xi}{1+\xi}\right)^{1/5}, \qquad \tilde{f}'(0,\xi) = 0, \qquad \tilde{\theta}(0,\xi) = 1,$$
$$\tilde{f}'(\infty,\xi) = (1+\xi)^{-2/5}, \qquad \tilde{\theta}(\infty,\xi) = 0, \qquad \tilde{h}(\infty,\xi) = 0. \tag{35}$$

It can clearly be seen that from the set of Eqs. (32) to (35) that the sets of Eqs. (9) to (12) and (16) to (19), appropriate for small and large ξ values, respectively, can easily be recovered.

As before, knowing the values of $\tilde{f}$ and $\tilde{\theta}$ and their derivatives, one can obtained the values skin friction and Nusselt number from

$$\frac{1}{2}Re^{1/2}C_f = (1+\xi)^{3/5}\tilde{f}''(0,\xi),$$
$$Re^{-1/2}Nu = -(1+\xi)^{1/5}\tilde{\theta}'(0,\xi). \tag{36}$$

Now, the solution of the non-similar system of Eqs. (32) to (35) is sought by implicit finite difference method. A brief discussion on this method is given below.

3.3.1. Implicit finite difference method

Finally, the solution for the complete range of ξ is sought by the implicit finite difference method, which was first introduced by Keller and Cebecci [19] and widely used by Hossain et al. [20].

Before we apply the aforementioned method, we first convert Eqs. (32) to (35) into a system of first order equations as

$$\frac{\partial\tilde{f}}{\partial\tilde{\eta}} = U, \qquad \frac{\partial U}{\partial\tilde{\eta}} = V, \qquad \frac{\partial\tilde{\theta}}{\partial\tilde{\eta}} = P, \tag{37}$$

$$V' + \tilde{f}V - U^2 + p_1(bU) + p_2\left(\frac{1}{2}b\tilde{\eta}V\right) + p_3(1-b) - p_4(2\tilde{h}) = p_2\left(\frac{5}{2}b\xi\frac{\partial U}{\partial\xi}\right), \tag{38}$$

$$\tilde{h}' = \theta, \tag{39}$$

$$\frac{1}{Pr}P' - 2U\tilde{\theta} + \tilde{f}P + p_2\left(\frac{1}{2}b\tilde{\eta}P\right) = p_2\left(\frac{5}{2}b\xi\frac{\partial\tilde{\theta}}{\partial\xi}\right), \tag{40}$$

$$\tilde{f}(0,\xi) = Sp_5, \qquad U(0,\xi) = 0, \qquad \tilde{\theta}(0,\xi) = 1,$$
$$U(\infty,\xi) = p_2, \qquad \tilde{\theta}(\infty,\xi) = 0, \qquad \tilde{h}(\infty,\xi) = 0, \tag{41}$$

where

$$p_1 = (1+\xi)^{-7/5}, \qquad p_2 = (1+\xi)^{-2/5}, \qquad p_3 = (1+\xi)^{-4/5},$$
$$p_4 = \xi/(1+\xi), \qquad p_5 = \{\xi/(1+\xi)\}^{1/5}. \tag{42}$$

We consider the net rectangle on $(\xi,\tilde{\eta})$ plane, denoted by the net points

$$\xi^0 = 0, \qquad \xi^m = \xi^{m-1} + k_m, \quad m = 1,2,3,\ldots,$$
$$\tilde{\eta}_0 = 0, \qquad \tilde{\eta}_j = \tilde{\eta}_{j-1} + l_j, \quad j = 1,2,3,\ldots,J, \tag{43}$$

where m and j are just the sequence of points on the $(\xi,\tilde{\eta})$ plane, and l_j and k_m be the variable mesh widths. We approximate the quantities $(\tilde{f}, U, V, \tilde{\theta}, P, \tilde{h}, Q)$ at the net points of the net by $(\tilde{f}_j^m, U_j^m, V_j^m, \tilde{\theta}_j^m, P_j^m, \tilde{h}_j^m, Q_j^m)$, which we call net function. If we assume $\tilde{f}_j^{m-1}, U_j^{m-1}, V_j^{m-1}, g_j^{m-1}, P_j^{m-1}, Q_j^{m-1}$ are known for $0 \leqslant j \leqslant J$, Eqs. (37)–(41) for a system of $6J+6$ equations for solution of $6J+6$ unknowns. This system of non-linear algebraic equations is linearised by Newton's method. The coefficient matrix thus formed has a block tri-diagonal structure. Such a system is solved using a block matrix version of well-known Thomas algorithm. This whole procedure of reduction to first order form followed by central difference approximations, Newton's quasi-linearisation method and block Thomas algorithm is well known as Keller Box method of Keller [21].

To initiate the process, we first prescribe the guess profile for the functions f and θ and their derivatives, at the starting time ($\xi = 0.0$). These profiles are then incorporated to the Keller Box scheme to march step by step in time of ξ values.

4. Results and discussion

In this study, an unsteady mixed convection flow over a heated porous surface is analysed inside a squeezing channel. The free stream velocity in the presence of squeezing channel surface is considered as a function of x and t. The analysis also include the effect of transpiration through the porous surface. The results are presented for a range of emerging parameters Pr, ξ, b and S. The solution of the problem is carried out for different range of ξ, *i.e.*, for small, large and entire ξ regime. Implicit finite difference method is used for solution of small and all ξ regimes. In addition to that, an asymptotic series solution is found for large ξ regime. To the authors best knowledge, no experimental results are available for such model, to compare the results with, however, this study can be of help for the experimentalists to carry out such work.

A comparison of the calculated numerical values of skin friction and heat transfer coefficients for different range of ξ, taking values of b equal to 0.2 and 0.5, are presented in Tables 1 and 2. A reasonably good agreement is observed between the results obtained by other methods. It can also be observed from the same tables, that for large values of ξ, the effect of b on the values of both $\frac{1}{2}Re^{1/2}C_f$ and $Re^{-1/2}Nu$ diminishes. This is very much expected, if look at the assumed potential flow that diminish at large time; at this stage flow develops solely due to the presence of buoyancy force and the flow is steady natural convection flow. It is further observed from the same tables that both the skin friction and heat transfer coefficients increase with the increase of time.

The numerical values of skin friction and heat transfer coefficients against the squeezing index b, for different values of ξ, are presented graphically in Fig. 2, for $Pr = 0.71$ and $S = 0.0$ (for a solid sensor surface). It is observed that value of $\frac{1}{2}Re^{1/2}C_f$ decrease as b increases, but it increases with increase in ξ. It is also interesting to notice that at some fixed value of ξ, there is an onset of reverse flow corresponding to some value of squeezing index b, for example, for $\xi = 1$, the onset of reverse flow occurs at $b = 3.75$. Similarly, for $\xi = 2$ and 3 the reverse flow occurs at $b = 4.15$ and 4.45, respectively.

The $\frac{1}{2}Re^{1/2}C_f$ and $Re^{-1/2}Nu$ against ξ for different values of Pr (equal to 0.71 for air 20 °C at 1 atm., 1.02 for water vapour at 140 °C, 6.7 for saturated water at 22 °C and 9.4 for water at 10 °C) are presented in Fig. 3, where values of squeezing index, b, and porosity parameter, S, are taken 0.5 and 0.0 respectively. It can be seen from this figure that for smaller values of Pr, skin friction coefficient is enhanced and Nusselt number is reduced. As we know that for smaller value of Pr, that corresponds to higher conductivity of the medium, the thermal buoyancy force increases. There is, thus, a growth in the fluid pressure both in x and y direction, which enhances the velocity in the immediate vicinity of heated surface and hence $\frac{1}{2}Re^{1/2}C_f$ increases. For the effect of Pr on $Re^{-1/2}Nu$, we borrow the same argument that, for smaller value of Pr, the effect of heated surface is transmitted deeper into the medium, thus giving a reduced heat transfer coefficient.

The effects of transpiration on the skin friction and heat transfer coefficients are expounded in Fig. 4. The positive value of S, represents the suction or withdrawal of fluid from the surface and negative value correspond to injection or blowing through the surface. The observation is that the injection enhances the skin friction, $\frac{1}{2}Re^{1/2}C_f$, and withdrawal suppresses it. Whereas, the effect of porosity on the Nusselt number is opposite, i.e. the injection reduces the Nusselt number, $Re^{-1/2}Nu$, and it increases due to suction through the surface.

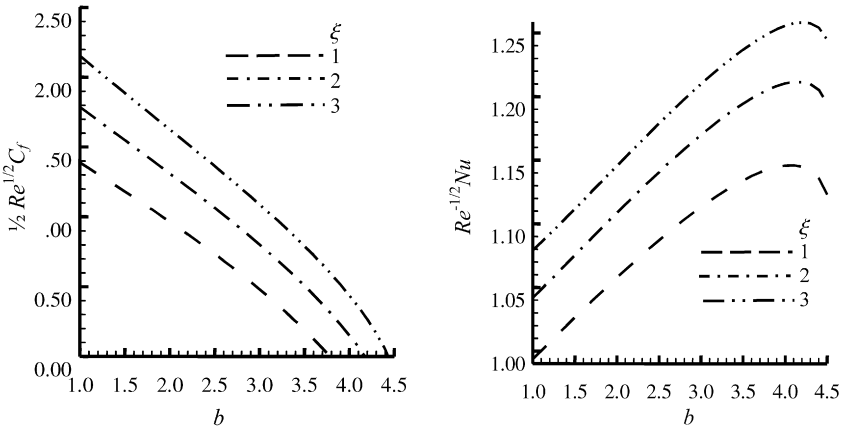

Fig. 2. Skin friction and heat transfer coefficients against b for different ξ, when $Pr = 0.71$, $S = 0$.

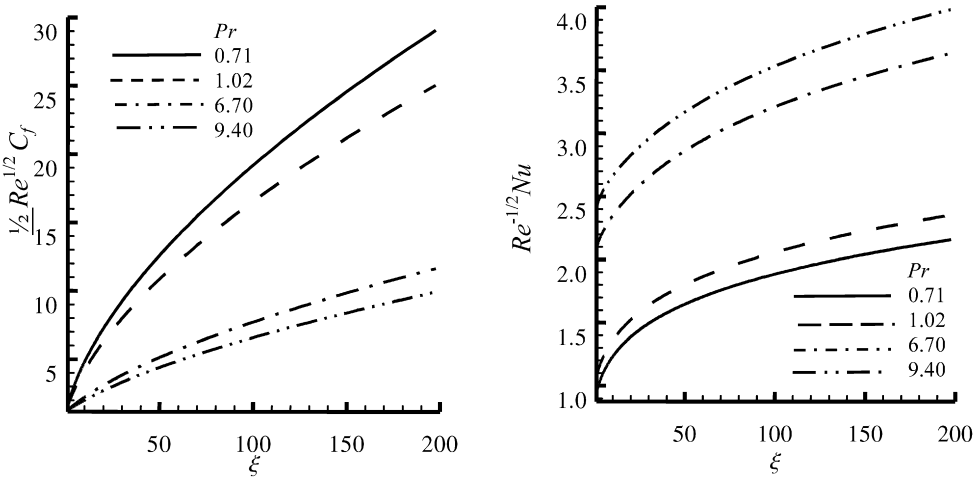

Fig. 3. Skin friction and heat transfer coefficients against ξ for different Pr when $b = 0.5$ and $S = 0$.

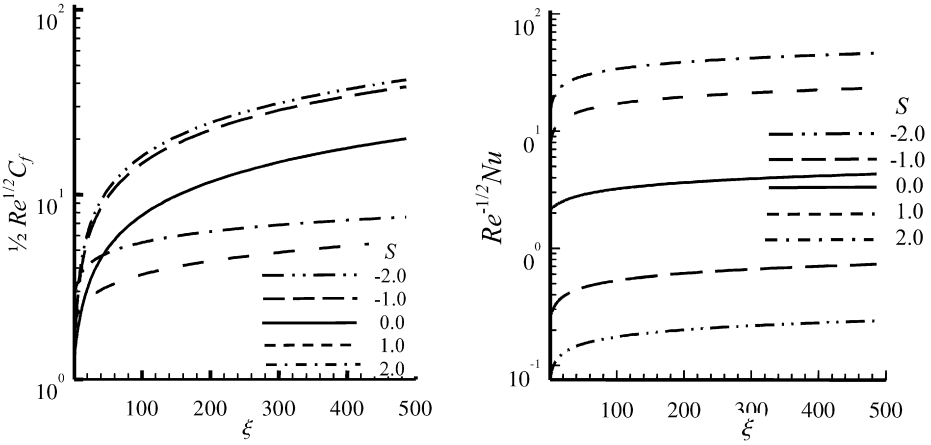

Fig. 4. Skin friction and heat transfer coefficients against ξ for different S when $b = 0.5$ and $Pr = 0.71$.

After discussion on effect of different physical parameter appearing in the problem, on skin friction coefficient, $\frac{1}{2}Re^{1/2}C_f$, and heat transfer coefficient, $Re^{-1/2}Nu$, we now see the effect of these physical parameters on velocity and temperature profiles. Fig. 5 explains the effect of ξ on the velocity profile, when values of b and Pr are assumed to be 0.5 and 0.71, respectively, for a rigid surface. It is quite interesting to observe that for smaller values of ξ, the flow corresponds to a forced convection flow, but as ξ increases, *i.e.*, with the lapse of time, the buoyancy effects come into play and the flow transforms to mixed convection flow. For extremely large value of the mixed convection parameter ξ, the buoyancy force becomes the main driving force and flow behaves like the natural convection flow. At the same time, we can see that for sufficiently large value of time the free stream velocity tends to zero and thermal buoyancy force becomes the only driving force for the flow. The dashed line in the figure shows the asymptotic veloc-

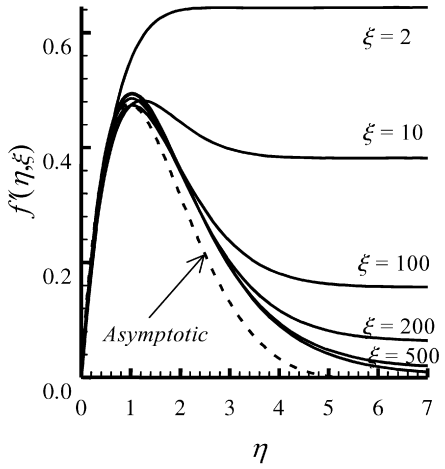

Fig. 5. Velocity profile for different ξ when $b = 0.5$, $Pr = 0.71$.

ity profile for extremely large time (solution of Eqs. (21) to (24)) and we can see that the solid lines are approaching the asymptotic profile with increase of ξ.

As already mentioned, for convective flows the momentum and energy equations are coupled, so we see the effect of Pr on velocity profile along with that on temperature profile. The effect of Pr on velocity and temperature profile for different values of ξ, when $b = 0.5$ and $S = 0.0$, is presented in Fig. 6. The effect of Pr on velocity profile is more pronounced for larger value of ξ. This is because, as ξ increases, the free stream velocity get smaller and the effect of buoyancy force becomes more pronounced. Also, we see that for smaller Pr, there is velocity overshoot near the heated surface, because for small Pr the conductivity of the fluid being high, there are greater density gradients, giving stronger buoyancy force. From the same figure we see that temperature is higher for smaller Pr number, due to high conductivity of the medium. The thermal boundary layer increases as Pr gets smaller value. Also, for the same Pr number, the temperature is small for small ξ and it increases as ξ increases. The thermal boundary layer is small for small ξ, because for small ξ, the free stream velocity is stronger and for the same conductivity of the medium (same Pr number), the effect of the heated surface carried into the medium is small.

The effect of surface porosity on velocity and temperature profiles is discussed in Fig. 7. It is observed that the effect of surface porosity is more prominent for larger ξ. This is because for large ξ the thermal buoyancy force is strong and injection or suction through the surface largely affects the flow pattern. Also we see that injection through the surface enlarges both the thermal and momentum boundary layer, whereas suction results in shrinking of both.

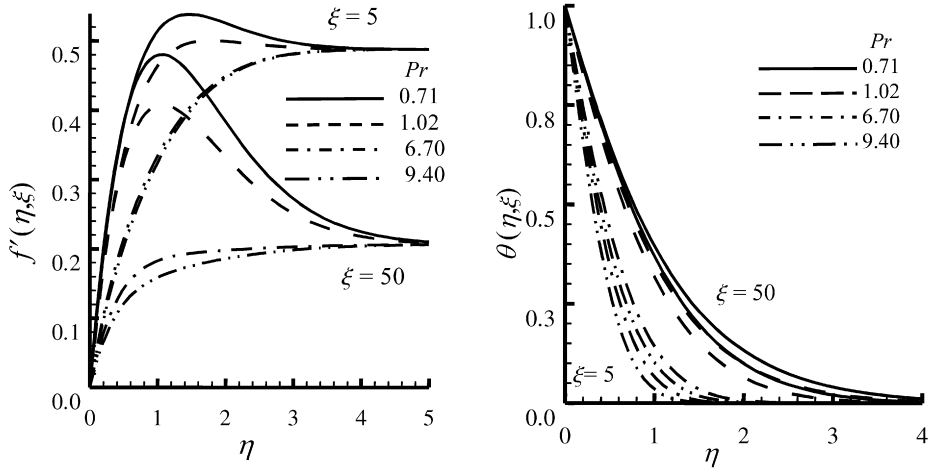

Fig. 6. Velocity and temperature for different ξ and Pr, when $b = 0.5$ and $S = 0$.

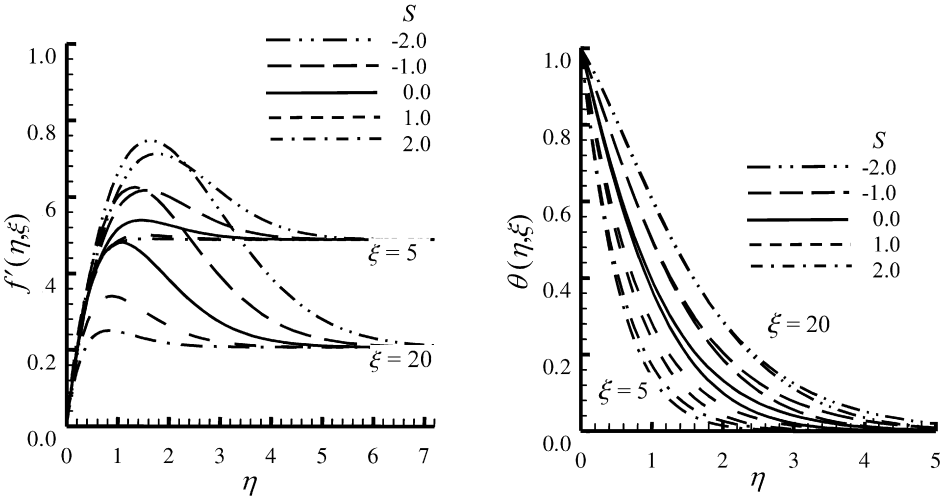

Fig. 7. Velocity and temperature for different ξ and S when $b = 0.5$ and $Pr = 0.71$.

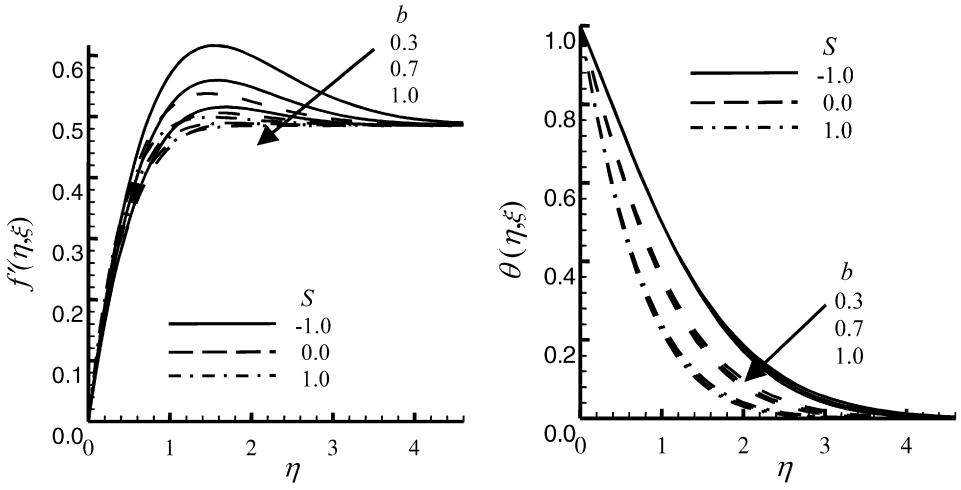

Fig. 8. Velocity and temperature for different S and b when $\xi = 5$ and $Pr = 0.71$.

The effect of squeezing index b, on velocity and temperature profile is explained in Fig. 8, for three values of S. The effect of b is more visible on velocity than on temperature. Increase in b results in shortening the momentum boundary layer, because with the increase in b, we can see that the free stream velocity reduces in magnitude. Also we see that when the fluid is injected through the surface the velocity profile is greatly affected with the variation in b.

5. Conclusions

In this paper we have analysed the unsteady mixed convection flow over a horizontal porous surface, inside a squeezing channel. The thermal buoyancy force is taken as the source of convective flow. The implicit finite difference and asymptotic methods are used for solution in different time regimes. The skin friction coefficient, heat transfer coefficient, velocity and temperature profiles are drawn for different values of the physical parameters involved. In the light of present investigations following conclusions may be drawn.

- In the beginning of time the flow is forced convection flow and as time lapses or the squeezing of the surface increases, there is a transition to the mixed convection flow, ending up with purely natural convection flow for extremely large value of time.
- Both the skin friction and heat transfer coefficients increase with increase in time and for large time the effect of squeezing index, b, on skin friction and heat transfer coefficients diminishes.
- The reverse flow at the horizontal surface starts at a certain limiting value of time as we go on squeezing the surface and the phenomenon occurs at higher degree of squeezing as we increase the time.
- At any time the skin friction coefficient is higher for smaller value of Pr number, and heat transfer coefficient is small when the value of Pr number is small.
- Transpiration greatly affects the flow and heat transfer behaviour. Suction at the surface increase the skin friction coefficient and decrease the heat transfer coefficient. The viscous boundary layer thickness decreases with suction, whereas, the thermal boundary layer increases with suction.
- For smaller Pr number the velocities are higher due to stronger buoyancy force and the temperature are higher due to higher thermal conductivity of the medium. Increase in Pr number, decreases the thermal boundary layer.

References

[1] Y. Mori, Buoyancy effects in forced laminar convection flow over a horizontal plate, J. Heat Transfer 83 (1961) 479–482.
[2] E.M. Sparrow, W.J. Minkowycz, Buoyancy effects of horizontal boundary layer flow and heat transfer, Int. J. Heat Transfer 5 (1962) 505–511.
[3] C.A. Hieber, Mixed convection above a heated horizontal surface, Int. J. Heat Mass Transfer 16 (1973) 769–785.
[4] L.G. Leal, Combined forced and free convection from a horizontal flat plate, 2, Z. Angew. Math. Phys. 24 (1973) 20–42.
[5] O.G. Martynenko, Yu.A. Sokovishin, Heat Transfer in Mixed Convection Flow, Nauka i Technika, Minsk, 1975 (in Russian).
[6] T.S. Chen, E.M. Sparrow, A. Mocoglu, Mixed convection in boundary layer flow on a horizontal plate, J. Heat Transfer 99 (1977) 66–71.
[7] A. Mocoglu, T.S. Chen, Mixed convection on a horizontal plate with uniform heat flux, in: Proc. 6th Int. Heat Transfer Conf. Hemishpere, Washington, vol. 1, 1978, pp. 85–90.
[8] X.A. Wang, An experimental study of mixed, forced and free convection heat transfer from a horizontal flat plate to air, J. Heat Transfer 104 (1982) 139–144.
[9] A. Moutsoglou, T.S. Chen, K.C. Cheng, Vortex instability of mixed convection flow over a horizontal flat plate, J. Heat Transfer 103 (1981) 257–261.
[10] L. Pera, B. Gebhart, Natural convection boundary layer flow over horizontal and slightly inclined surface, Int. J. Heat Mass Transfer 16 (1973) 1131–1146.
[11] W. Schneider, A similarity solution for combined forced and free convection flow over a horizontal plate, Int. J. Heat Mass Transfer 22 (1979) 1401–1406.
[12] M.S. Raju, X.Q. Liu, C.K. Law, A formulation for combined forced and free convection past horizontal and vertical surfaces, Int. J. Heat Mass Transfer 27 (1984) 2215–2224.
[13] W. Schneider, M.G. Wasel, Breakdown of the boundary layer approximation for mixed convection above a horizontal plate, Int. J. Heat Mass Transfer 28 (1985) 2307–2313.
[14] N. Afzal, Mixed convection in buoyant plumes, in: Handbook of Heat and Mass Transfer Operations, Gulf Texas, 1985 (Ch. 37).
[15] H. Steinrück, Mixed convection over a cooled horizontal plate: non-uniqueness and numerical instabilities of the boundary-layer equations, JFM 278 (1994) 251–265.
[16] J.P. Denier, P.W. Duck, J. Li, On the growth (and suppression) of very short-scale disturbances in mixed forced-free convection boundary layers, JFM 526 (2005) 147–170.
[17] M. Mahmood, S. Asghar, M.A. Hossain, Squeezed flow and heat transfer over a porous surface for viscous fluid, Heat Mass Transfer 44 (2007) 165–173.
[18] A. Khaled, K. Vafai, Hydromagnetic squeezed flow and heat transfer over a sensor surface, Int. J. Engg. Sci. 42 (2004) 509–519.
[19] H.B. Keller, T. Cebecci, Accurate numerical methods for boundary-layer flows. Part I, Two dimensional laminar flows, in: Proceedings of the International conference on Numerical Methods in Fluid Dynamics, in: Lecture Notes in Physics, Springer, 1971.
[20] M.A. Hossain, Sidharta Bhomick, R.S.R. Gorla, Unsteady boundary layer mixed convection flow along a symmetric wedge with variable surface temperature, Int. J. Engg. Sci. 44 (2006) 607–620.
[21] H.B. Keller, Numerical methods in boundary layer theory, Annu. Rev. Fluid Mech. 10 (1978) 417–433.